African Journal of Biological Sciences


# Interaction Behavior of Novel Chitosan-Pectin Complex of Ciclopirox with Human Galectin-3: Molecular Docking, Molecular Dynamic Simulation, *In Silico* Pharmacokinetics Studies

***Dr Savita Deokar[1], Dr. Karimunnisa Shaikh[2*], Dr.Sangita Abasaheb Kale[3], Dr. Dipali M. Dhoke[4], Ms. Saniya Sameer Shaikh[5], Ms.Saakshi Shrikant Deokar[6]***

[1]PCET's School of Pharmacy, Pimpri Chinchwad University (PCU), Sate, Maval (PMRDA) Dist.,Pune-412106,Email: savita.deokar@pcu.edu.in

[2*]PES's Modern College of Pharmacy, Nigdi, Pune, Maharashtra, India, Email:karima78@rediffmail.com

[3]Department –Pharmaceutics, PES's Modern College of Pharmacy, Nigdi, Pune, Maharashtra, India

[4]JSPMs Charak College of Pharmacy and Research,Wagholi, Pune.

[5]Poona College of Pharmacy, Bharati Vidyapeeth, Erandawane, Pune

[6]PES's Modern College of Pharmacy .Nigdi, Pune,Maharashtra, India

***Correspondence address:** Dr. Karimunnisa Shaikh

*Email:karima78@rediffmail.com

Article History
Volume 6, Issue Si4, 2024
Received: 25 May 2024
Accepted: 15 June 2024
Published: 05 July 2024
Doi: 10.48047/AFJBS.6.Si4.2024.
951-963

**ABSTRACT**

In variety of epithelial cancers, Galectin-3, a beta-galactoside-binding protein, has been observed to be overexpressed. Ciclopirox (CPX) is an antifungal medicine that treats mycoses of the skin and nails. Our research group previously investigated the repurposing of CPX as an anti- colon cancer agent. The study demonstrated that CPX effectively inhibited six drug targets: Cell Division Cycle 25A (Cdc25A), Protein Deglycase DJ-1 (DJ-1), Retinoblastoma Protein (p-Rb/Rb), Cyclin-Dependent Kinase-4 (CDK4), High-Mobility Group AT-Hook-2 (HMGA2), and Catenin β-1 (Wnt/β-catenin). However, following analysis of various pharmaceutical databases such as Science Direct, PubMed, Google Scholar, and others, it was hypothesized that the interaction of ciclopirox-chitosan-pectin (CPX-CHT-PEC) complex (produced by complexing CPX with chitosan and pectin via polyelectrolyte complexation technique) against galectin-3 was not studied yet. This study's prime aim was at investigating the possibilities of novel CPX-CHT-PEC complex as an agent for anti-colorectal cancer with utilization of *in-silico* techniques against the target galectin-3 using Schrodinger Maestro Software suite 2021-2. Furthermore, the drug-likeness, bioavailability, drug targets, and pharmacokinetics of the CPX-CHT-PEC complex were predicted with the help of online computational tools such as SwissADME and SwissTarget Prediction. The *in-silico* analysis suggested that the novel CPX-CHT-PEC complex could play a significant role in managing colon cancer by effectively inhibiting the molecular target galectin-3.The pharmacokinetics, bioavailability, and drug-likeness characteristics of both ligands further reinforced their potential for lead development. The study will therefore provide insights into the application of this complex for the scientists, doctors, chemists, and other healthcare persons in the view of evolving challenges in chemotherapeutics.

**INTRODUCTION**

The LGALS3 gene is responsible for the production of the galectin-3 protein in human beings. Galectin-3, belonging to the lectin family, comprises of 14 different mammalian galectins that was discovered so far. Galectin-3 which is of 30 kDa molecular weight, and, like all other galectins, comprises of carbohydrate-recognition-binding domain and consists about 130 amino acids [1]. This domain allows the galectin to bind specifically to beta-galactosides. Galectin- 3 belonging to the family of beta-galactoside-binding protein, also acts as a crucial factor in cell-cell adhesion, interactions between cells and their matrix, activation of macrophages, angiogenesis, metastasis, and death. One gene, LGALS3, which is situated on chromosome 14 at the location q21–q22, is responsible for encoding galectin-3. Galectin-3 may be found expressed on the surface of the cell, and also in the nucleus, cytoplasm, mitochondria, and extracellular space [2].

Galectin-3 is a beta-galactoside-binding protein, is observed to be overexpressed in a variety of epithelial cancers [3]. These cancers encompass colorectal, breast, lung, prostate, pancreatic, head and neck, and melanoma. Elevated galectin-3 expression is frequently related with metastasis development and unfavorable prognosis [4]. Cancer patients, and especially cancer patients who have metastases, have been shown to have higher levels of the circulating galectin-3 [5]. Overexpression of galectin-3 has been demonstrated in a number of studies to promote numerous processes in progression and spread of cancer, comprising cell adhesion with invasion, angiogenesis, new blood vessels establishment and suppression of immune responses [6]. The ability of galectin-3 to glycoproteins to bind to the surface of the cell that terminate with galactoside has been found to be connected with a significant number of galectin-3's activities that promote the development of cancer. For instance, attachment of galectin-3 to the oncofetal Thomsen-Friedenreich Gal1,3GalNAc-Thr/Ser (TF antigen) upon mucin protein's transmembrane MUC1 [7] strengthen the circulation of tumor cell homotypic clustering and survival [8] and enhances attachment of circulating tumor cell to vascular endothelium [9]. Increased production of the IL-6 and G-CSF which are metastasis-promoting cytokines, may be assigned to the binding of CD146 to galectin-3 on the endothelial cell's surface through N-linked glycans [10]. It is hypothesized, based on the widespread effect that galectin-3 has on the contribution of cancer development, that the overexpression of galectin-3 and the secretion of it by cancer cells may have an effect on the cellular secretion of proteases, and as a result, may contribute to the invasion and metastasis of tumor cells.

Ciclopirox (CPX) is an antifungal medicine that treats mycoses, a fungal infection of the skin and nails. It is synthetic, has a wide range of activity, and is no longer under patent protection. It is applied to the skin in order to prevent fungal infections, and it may be found in a number of different formulations, such as gels, creams, lacquers, topical solution, and shampoos [11]. It possesses an advantage that no other oral anti-mycotic medication has, and that advantage is in the form of a superior benefit-to-risk ratio. This is due to the fact that CPX is very well tolerated, and it has no serious side effects whatsoever [12]. It was recently discovered that CPX has significant potential effectiveness against a range of disorders, including cancer, and that it has an excitingly powerful anti-proliferative impact on tumor cells [13]. It has been recently discovered to be comprised of anticancer activity *in vitro* and *in vivo*, and it is under Phase-I study for research in patients who have relapsed or are resistant to treatment for hematologic malignancies [14]. However, with regard to the use of CPX, the repurposed molecule for Colo-rectal cancer (CRC) treatment, and more specifically the molecular targets, has received a comparatively low amount of attention up to this point.

Drug repurposing, referred to as drug repositioning, re-profiling, or re-tasking, incorporates new methods for accepted or investigating drugs that extend beyond their original medical indications. This method presents many advantages compared to developing entirely new medications for specific conditions. As repurposed pharmaceutical shows to be quite attentive in preclinical models and in humans, provided that early-stage studies have been done previously, it is rarely unsuccessful in the future trials for efficacy, at the minimum standpoint of its safety profile [15]. Second, although though the most cases of the preclinical research, safety evaluations, and, in certain instances, formulation development may have

already been finalized, potentially shortening the drug development timeline [16]. Third, fewer assets are required, which may differ greatly hinging on the stage the candidate for repurposing is at in the development process and the stage they were previously in. Although the expenses associated with regulatory and phase-III testing for a repurposed pharmaceutical could be similar to those for a new drug targeting the similar direction, costs related to preclinical, phase-I, and phase-II testing may be notably lower [17].

Earlier, we documented the repurposing of CPX as an anti-colon cancer agent, demonstrating its effective inhibition of six drug targets, including Cell division cycle 25A (Cdc25A), Protein deglycase DJ-1 (DJ-1), Retinoblastoma protein (p-Rb/Rb), Cyclin-dependent kinase-4 (CDK4), High-mobility group AT-hook-2 (HMGA2), and Catenin β-1 (Wnt/β-catenin) [18, 19]. However, post searching multiple databases of pharmaceuticals like as ScienceDirect, PubMed, Google Scholar, and others, as chitosan and pectin have its own and combined therapeutic effect to inhibit colon cancer [20], it was hypothesized that the interaction of ciclopirox-chitosan-pectin (CPX-CHT-PEC) complex (produced by complexing ciclopirox with chitosan and pectin via polyelectrolyte complexation technique) against galectin-3, as it is not studied yet. The prime aim of this research was to understand the prospective of novel CPX-CHT-PEC complex as an agent for anti-colorectal cancer by utilizing *in-silico* approaches against the targetgalectin-3 using Schrodinger Maestro Software suite 2021-2. Furthermore, online computational tools (SwissADME and SwissTargetPrediction) have been utilized to predict the drug-likeness, bioavailability, drug targets, and pharmacokinetics of the CPX-CHT-PEC complex.

## MATERIALS AND METHODS

### Molecular docking study

**Ligand Preparation:** Schrodinger Software suite 2021-2's 2D-sketcher module was used to create structures and Maestro environment version 12.8 was used to perform docking analysis. LigPrep Programme was used to prepare stereoisomers of these ligands. For each ligand, Epik ionizer, up to four poses were generated with correct protonation states at a pH of 7.0 for the target. The OPLS 2005 force field generated desalted, tautomerized ligands while preserving the necessary chiralities from the input files, resulting in an optimized 3D ligand with low energy. [21].

**Protein Preparation:** Human galectin-3 CRD protein crystal structure (PDB ID:6Q0Q) was chosen as prime target retrieved from RCSB Protein Data Bank (PDB). Maestro 9.1's Protein Preparation Wizard was used to make produce protein structures. To create biological targets, pre-processed and validated structures were used. In order to achieve the correct conformation, disulfide bonds, bond orders, and formal charges, Protein Preparation Wizard module of the Schrodinger Maestro 9.1 was use do-factors, metal ions, water molecules beyond a 5Å distance from the crystal formation, and hetero groups were all eliminated. To optimize hydrogen atoms preserving all heavy atoms in their original positions,"impref utility" tool was applied while to optimize Hydrogen bonding network, "H-bond assignment" tool was used. Molecular docking was employed to highlight receptor grids based on the protein structure, enabling the exploration of various ligand poses binding to the predicted active site. Around the ligand's centroid to encompass the entire ligand within a cubic box of specified dimensions, characterized by a Van der Waals scale factor of 1.00 and a charge cutoff of 0.25, grids were constructed and aligned. XP mode was used to perform docking and using energy-minimized conformations grid line scores were evaluated. The most favorable docking comprises with the lowest Glide score value was selected for every ligand following the docking of the top-scoring ligands. [22].

**Induced-Fit Molecular Docking:** After understanding the target protein structure, drug designing process was begun. Docking with the low-energy ligands for stiff receptors was done, and evaluation was done for its fit into the active site and predicted binding mechanism. The interaction between the ligand and the macromolecule protein (receptor) was

modeled with the help of molecular docking techniques with receptor-based computational methods. This method contributes in identifying low-free-energy structures and also allows in complete removal of steric conflicts. With 0.7 Van der Waals scaling and 0.5 Van der Waals for receptor and scaling for the ligand respectively, elimination of side chain ligands were done, and a 0.18 RMSD value cut off, the maximum number of comprises for every individual ligand remained at 20. Using a Van der Waals scaling of 0.7 for the receptor and 0.5 for the ligand, side chains were excluded, and a cut-off of 0.18 RMSD was applied, allowing a maximum of 20 poses per ligand. For each ligand, according to the obtained ranked scores, glide scores were assigned [23].

**Studies of Pharmacokinetics, Bioavailability, and Drug-likeliness:** Using SwissADME online tool, prediction research of pharmacokinetics, namely ADME, bioavailability, and drug-likeness of ligands were done. Six physicochemical properties were used to assess drug-likeness, which calculates bioavailability radar: lipophilicity, molecular size, polarity, insolubility, flexibility, and unsaturation. The properties of ADME such as passive human gastrointestinal absorption (HIA), permeability to blood-brain barrier and glycoprotein (P-gp) substrate status, were assessed as positive or negative using the BOILED-Egg model within the tool. The calculation of lipophilicity (Log P/w) parameters involves iLOGP, determined using the GB/SA model based on solvation energies in n-octanol and water. XLOGP3 employs an atomistic method with adjustments from a knowledge-based library, WLOGP utilizes a purely atomistic approach, and MLOGP relies on a topological method. The original rule-of-five implemented in a tool, was employed for predicting drug-likeness using the Lipinski (Pfizer) filter. According to several physicochemical characteristics oral bioavailability was analyzed using the bioavailability radar. The parameters were specified as follows: LIPO (lipophilicity) with XLOGP3 ranging from -0.7 to +5.0; SIZE (molecular weight) between 150 g/mol and 500 g/mol; POLAR (polarity) with a TPSA (topological polar surface area) ranging from 20 Å² to 130 Å²; INSOLU (water insolubility) by log S scale, where Logs (ESOL) falls between 0 and 6; INSATU (in saturation) or saturation based on the fraction of carbons in sp3 hybridization, where Fraction Csp3 ranges from 0.3 to 1; and FLEX (flexibility) determined by the number of rotatable bonds, which ranges from 0 to 9 [24].

**Identification of Drug Targets:** A web service known as Swiss Target Prediction, was used for the forecasting of small molecules that are bioactive and allows for predicting tine molecule targets. The query molecules are evaluated against a database of 280,000 compounds active across over 2000 targets in five different species with the help of 2D and 3D similarity measures. To comprehend the molecular mechanisms underlying bioactivity and predict potential side effects or cross-reactivity, it is essential to map the targets of tiny molecules that are bioactive. Using three different organism models, predictions were made and mapping predictions through homology allows for the identification of targets among closely related paralogs and orthologs within and across species. Inhibitory targets for CPX-CHT-PEC complex were seen in all of these three models: The human (*Homo sapiens*), rat (*Rattus norvegicus*), and mouse (*Mus musculus*) [25].

**Molecular dynamic simulation:** A MD simulation was conducted to investigate the lead compound's binding stability in complex with the Human galectin-3 CRD crystal structure (PDB ID:6Q0Q) in dynamic conditions. Desmond module from the Schrödinger 2020-1 suite, deployed on an Ubuntu 18.04 system running on an HP Z2 G2 TOWER workstation featuring an NVIDIA Quadro 6000 4GB graphics processing unit (GPU) was used to perform MD simulations. On obtaining the Protein Preparation Wizard module, ligand–protein complexes solvated with the help of point charge (SPC) molecules of water, which are orthorhombic box with a minimum distance of 10A° from the protein surface to the box's sides. After completing the Protein Preparation Wizard module, the ligand-protein complexes were solvated with simple point charge (SPC) water molecules. The solvation was carried out in an orthorhombic box, ensuring a minimum distance

of 10 Å between the protein surface and the sides of the box. Counter ions (22Na+ and 30Cl-) were introduced using the system builder module to achieve electrical neutrality in each system. Additionally, salt (NaCl) was included at a concentration of 0.15M to mimic physiological conditions. The solvated system underwent energy minimization using a hybrid algorithm Broyden-Fletcher-Goldfarb-Shanno (LBFGS) methods in the OPLS3e force field. This process aimed to reduce steric clashes between the protein and solvated water molecules. The simulation was conducted in NPT ensembles (isothermal-isobaric) with trajectory snapshots taken at 100 ps intervals, running for a duration of 100 ns. Using the Nose-Hoover chain thermostat and Martyna-Tobias-Klein barostat controllers, respectively, a temperature of 300 K and pressure of 1 bar were maintained throughout the simulation [26].

## RESULTS AND DISCUSSION

**Molecular docking study:** CPX-CHT-PEC complex**(Figure 1A)**expressed significantly high inhibition (Gscore of -11.856 Kcal/mol) against the target galectin-3 by interacting with amino acid residues GLU165, ASN174, GLY182, GLU184 by forming 8 hydrogen bonds via hydroxyl, amine, and carbonyl groups. Also, a non-hydrogen bonding (π-π stacking) was observed through amino acid residue TRP181via aromatic component of the structure. The individual components such as CPX**(Figure 1B)**, CHS**(Figure 1C)**, and PEC **(Figure 1D)**demonstrated good inhibition the target with Gscore of -8.04Kcal/mol (interacting with the residues of amino acid such as GLN150and by forming 1 hydrogen bond via hydroxyl groups), -8.67Kcal/mol (interacting with the residues of amino acids like ARG144, ASP148, LYS176 by forming 4 hydrogen bonds via hydroxyl groups), and -7.92 Kcal/mol (interacting with amino acid residue ARG144, ASP148, LYS176by forming 5 hydrogen bonds via hydroxyl and carbonyl groups), respectively (**Table 1**).

**Table 1.** Docking score of compounds against the target galectin-3.

| Compound | Docking score (Kcal/mol) | Hydrogen bonding | Amino Acid residues | Van der Waals interactions |
|---|---|---|---|---|
| CPX-CHS-PEC | -11.856 | 8 | GLU165, ASN174, GLY182, GLU184 | TRP181 |
| CPX | -8.04 | 1 | GLN150 | - |
| CHS | -8.67 | 4 | ARG144, ASP148, LYS176 | - |
| PEC | -7.92 | 5 | ARG144, ASP148, LYS176 | - |

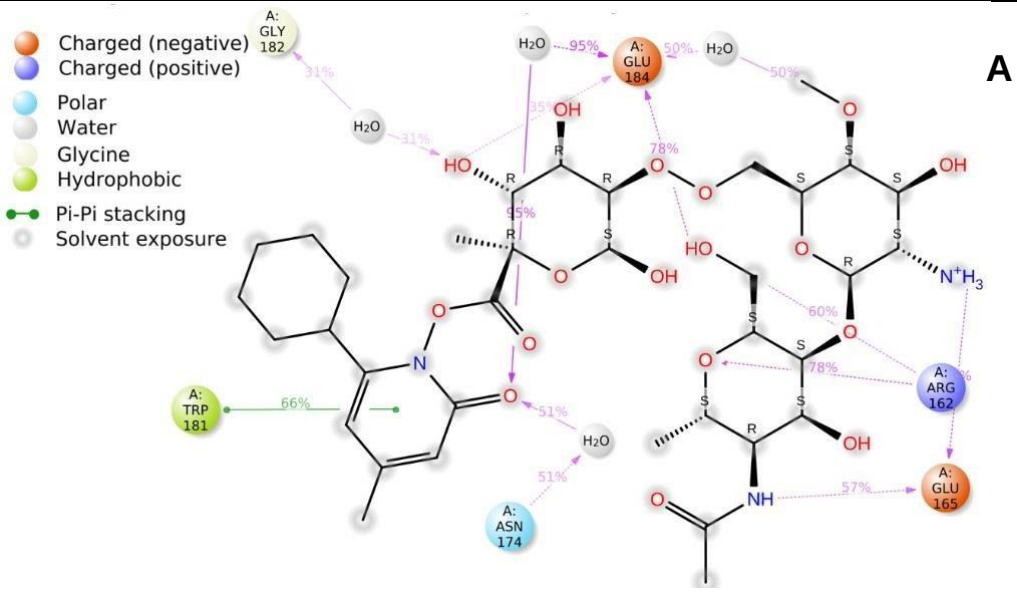

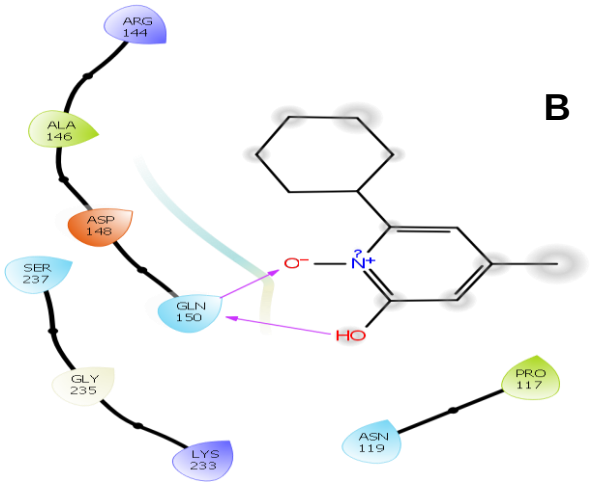
B
ARG 144
ALA 146
ASP 148
SER 237
GLN 150
GLY 235
LYS 233
PRO 117
ASN 119
HO

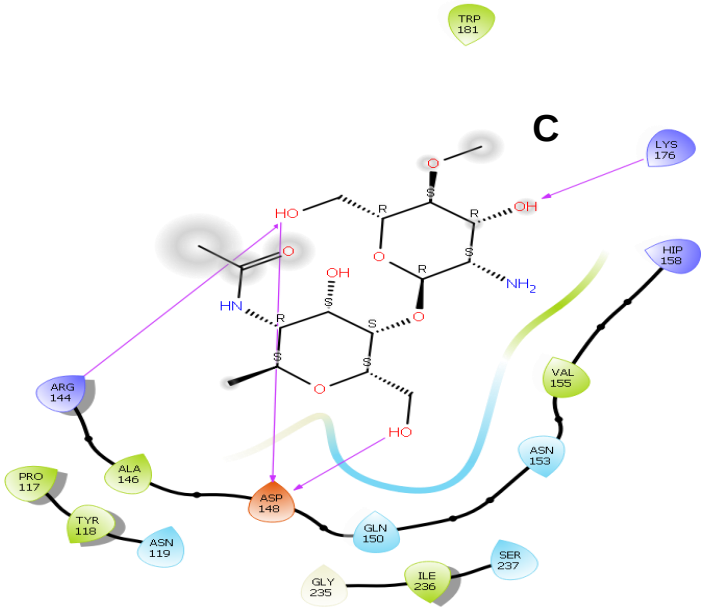
C
TRP 181
LYS 176
HIP 158
VAL 155
ASN 153
ARG 144
ALA 146
PRO 117
TYR 118
ASN 119
ASP 148
GLN 150
GLY 235
ILE 236
SER 237
HO
OH
NH2
HN

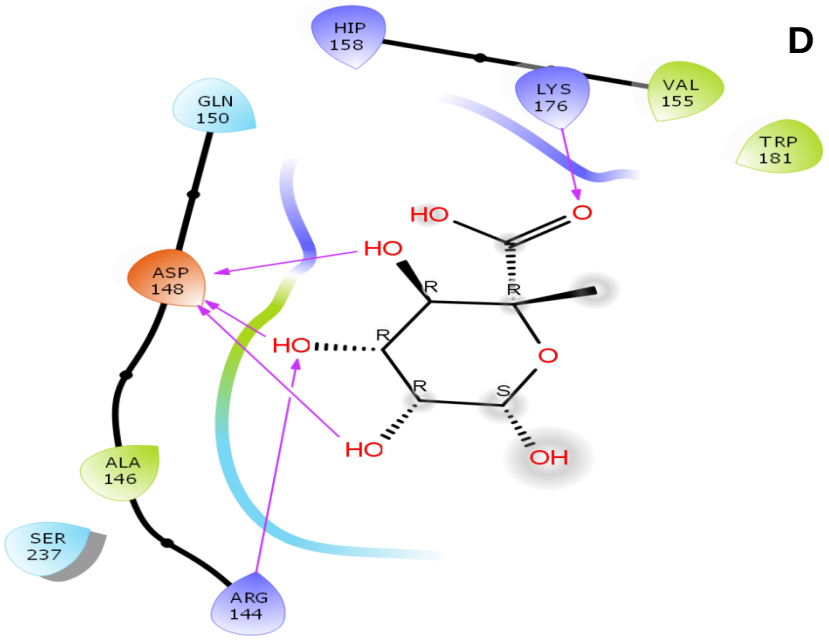


**Figure 1.** Docking poses of (A) Complex, (B) Ciclopirox, (C) Chitosan, and (D) Pectin.

**Molecular dynamic simulation:** To investigate the high-power properties of ligand-protein complex interactions, a molecular dynamic simulation was undertaken to understand the solidity of he bound form of the lead compound CPX-CHT-PEC in the binding site of 6Q0Q. Our simulations ran for up to 100 ns to assess the stability and changes in the conformation of the CPX-CHT-PEC-6Q0Q complex. This investigation further utilized a 100 ns duration, sufficient for determining the configurations of 6Q0Q Cα atoms when complexed with the lead compound CPX-CHT-PEC.

As shown in **Figure2A**, during the dynamics analysis, the stability of the protein ligand complex was calculated using the RMSD values of the protein Cα atoms. The expectation is that a lower RMSD value throughout the simulation indicates the protein-ligand complex stability. Conversely, a higher RMSD value suggests lower stability. Initially, the ligand RMSDs fluctuated between 0.4 Å and 1.6 Å during equilibration, stabilizing there after between 1.00 Å and 2.00 Å for the remainder of the simulation, with minor fluctuations observed towards the end, specifically between 90 and 100 ns. Also, it protein was seen to had moderate fluctuations of RMSD, ranging from 0.8Å to 1.6Å. Higher fluctuation is observed in initial 20-60ns time where RMSD is rises up to 1.6Å till 60ns after that RMSD goes down and maintain minor fluctuations throughout the simulation time that suggests lead compound CPX-CHT-PEC tightly attached to the cavity of 6Q0Q.

In **Figure2B,** Graphical representations are used to depict the root-mean-square fluctuation (RMSF) values of residue of the protein backbone. In these graphs, the peaks show that how much residue of every amino acid fluctuates throughout the whole simulation. Higher RMSF values shows greater residue flexibility, while lower RMSF values shows less flexibility and greater stability of the system. The RMSF plot indicates secondary structural elements highlighted with red for α-helices and blue for β-strands, while loops are represented in white. α-helices and β-strands typically show less fluctuation compared to unstructured protein regions, which contributes to their stiffness. If there was minimal fluctuation in the residues within the active site and main chain, it suggested that there was little conformational change, indicating that the identified lead compound was securely attached within the target protein's binding pocket. The protein backbone residues in the catalytic domain exhibit RMSF values ranging from 0.6 Å to 2.4 Å, showing higher changes in the C-terminal and N-terminal regions compared to other protein parts. The CPX-CHT-PEC compound was observed to relate with 36 amino acids of 6Q0Q, along with Gly112 (5.4Å)Pro113(3.3Å), Leu114(1.0Å), Thr133(0.4Å), Leu135(0.4Å),

Gly136(0.5Å), Thr137(0.4Å), Arg144(0.5Å), His158(0.4Å), Arg162(0.4Å), Asn164(0.6Å), Glu165(0.6Å), Asn166(1.0Å), Arg168(0.6Å), Asn174(0.4Å), Lys176(0.5Å), Asp178(1.1Å), Asn179(1.1Å), Asn180(0.9Å), Trp181(0.6Å), Gly182(0.6Å), Arg183(0.6Å), Glu184(0.4Å), Arg186(0.4Å), Gly195(0.6Å), Lys196(0.6Å), Pro197(0.5Å), Phe198(0.5Å), Lys199(0.5Å), Asn214(0.7Å), Asp215(0.7Å), Lys227(0.9Å), Asp241(0.5Å),

Thr243 (0.6Å), Ser244 (0.6Å), Ser246 (0.6Å). The RMSF value of less than 2.4 Å was observed in these interacting residues, and is shown with green vertical bars except GLY112.

In the analysis of 2D-ligand interaction, the polar groups like amino and protonated -NH groups predominantly engage in conventional hydrogen bonding and hydrogen bonding with the help of residues. The contract analysis of Protein-ligand reveals that residues Arg162, Glu165, and Glu184 participate in hydrogen interactions with the lead compound CPX-CHT-PEC (**Figure 2C**).At the time of MD simulation, Trp181 demonstrated significant hydrophobic interactions. Additionally, an ionic interaction was observed with Asn166 in the complex. Water-mediated hydrogen bonding further stabilized the potential compound CPX-CHT-PEC within the 6Q0Q binding cavity, involving various residues. (**Figure2D**).

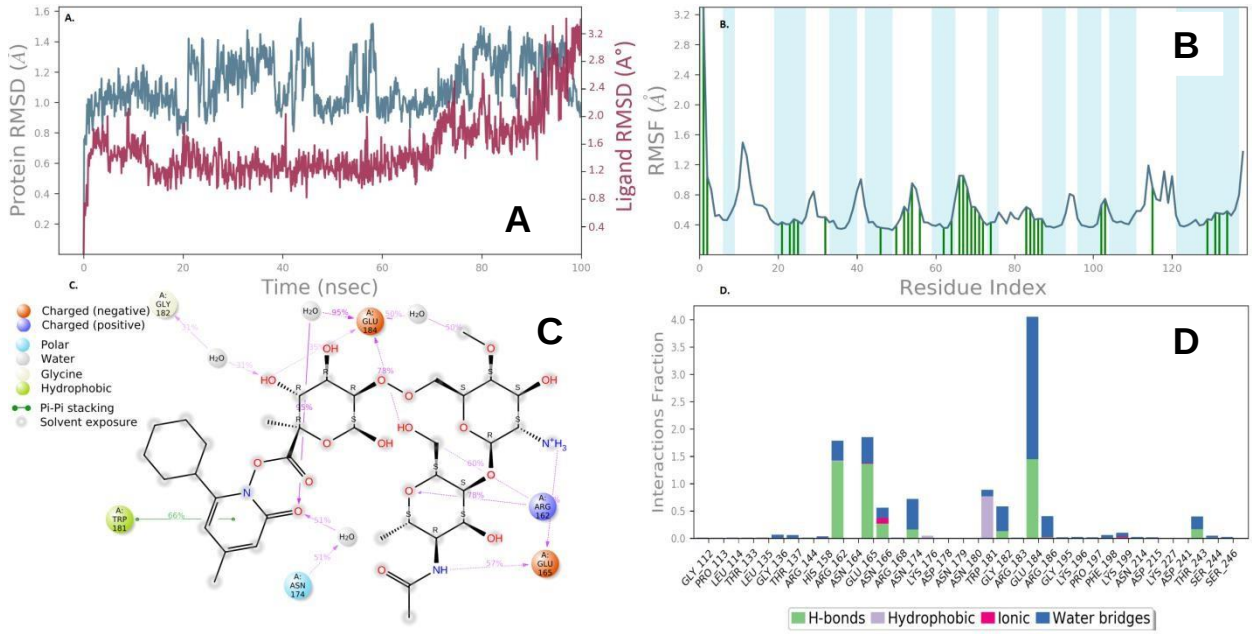


**Figure 2.**MD simulation analysis of CPX-CHT-PEC-6Q0Q complex (**A**) RMSD (Protein RMSD is shown in grey while RMSD of compound CPX-CHT-PEC are shown in red) (**B**) Protein RMSF (**C**) 2D Interaction diagram and (**D**) Protein–ligand contact analysis of MD trajectory.

**Pharmacokinetics, Bioavailability, and Drug-likeliness studies:** In the**Table 2**thedata of pharmacokinetics, bioavailability and drug-likeness and data on complex of CPX-CHT-PEC are shown. The molecule exhibited poor oral absorption, low gastrointestinal absorption, blood-brain negligible permeability, and minimal skin permeation. It was also identified as a neutral substrate for p-glycoprotein, and the complex did not act as a substrate for CYP1A2, CYP2C19, CYP2C9, CYP2D6, and CYP3A4 enzymes in the terms of metabolism. Drug-likeness studies indicated significant violations of Lipinski's rule of 5 as well as other rules (Ghose, Veber, Egan, and Muegge), suggesting challenges from both physicochemical and pharmacological perspectives.

While predicting the bioavailability, CPX-CHT-PEC received a low score of 0.17, indicating moderate predicted water solubility. The oral bioavailability radar indicated the following parameters: INSATU (unsaturation as per Csp3) was

0.80, FLEX (number of rotatable bonds) was 14, INSOLU (ESOL Logs) was -2.39, SIZE (molecular weight) was 678.63 g/mol **(Figure 3A)**, POLAR (total polar surface area, TPSA) was 289.41 Å², and LIPO (XLOGP3 value) was -2.39 (**Figure 3B**).

For the BOILED-Egg model (**Figure 3C**), CPX-CHT-PEC showed least ability of blood-brain barrier penetration along with lower gastrointestinal absorption capacity. The obtained molecule was neither PGP negative nor PGP positive as non-substrate in predictive model.

The BOILED-Egg method, (Brain or IntestinaLEstimateD permeation method) known for accurately predicting the lipophilicity and polarity of small molecules, has been proposed as an effective tool. Based on comprehensive predictive outcomes, CPX-CHT-PEC appears promising as per the bioavailability radar and BOILED-Egg analysis. Nevertheless, these predictive findings must undergo validation through in vitro and in vivo functional and pharmacological assays for colon cancer management.

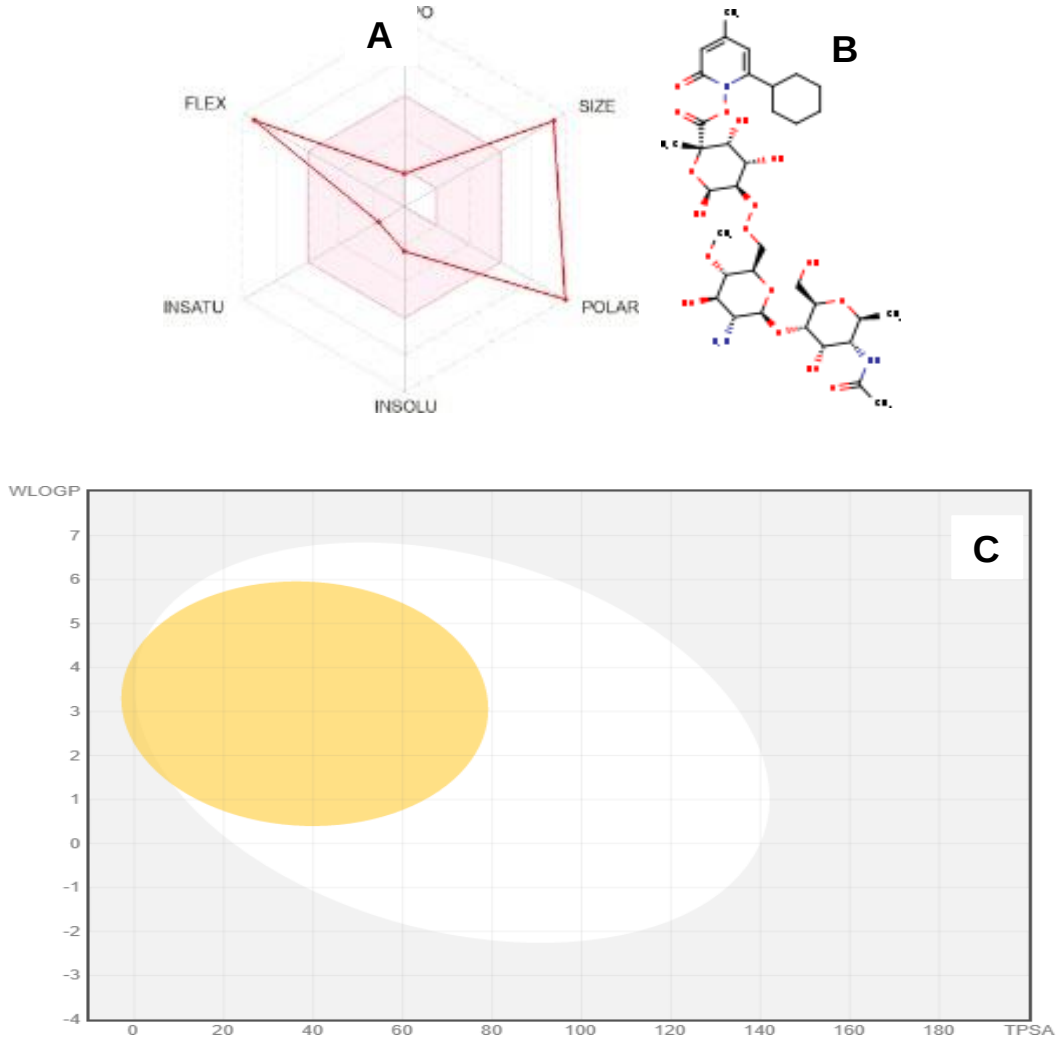


**Figure 3.**Pharmacokinetic predictions for CPX-CHT-PEC: (A) Chemical Structure, (B) Plot for Bioavailability radar, and (C) BOILED Egg Model.

**Table 2.** Pharmacokinetic and physicochemical characteristics of CPX-CHS-PEC.

| **PROPERTIES** | **DATA** |
|---|---|
| **Physicochemical Properties** | |
| Formula | $C_{35}H_{55}N_3O_{17}$ |

| | |
|---|---|
| Molecular weight | 789.82 g/mol |
| Number of heavy atoms | 55 |
| Number of aromatic heavy atoms | 6 |
| Fraction Csp3 | 0.80 |
| Number of rotatable bonds | 14 |
| Number of H-bond acceptors | 18 |
| Number of H-bond donors | 8 |
| Molar Refractivity | 184.92 |
| TPSA ($A^2$) | 289.41 |
| **Lipophilicity** | |
| Log Po/w (iLOGP) | 3.72 |
| Log Po/w (XLOGP3) | -2.39 |
| Log Po/w (WLOGP) | -3.24 |
| Log Po/w (MLOGP) | -2.68 |
| Log Po/w (SILICOS-IT) | -3.03 |
| Consensus Log Po/w | -1.52 |
| **Water Solubility** | |
| Log S (ESOL) | -2.39 |
| Solubility | 3.23e+00 mg/ml ; 4.09e-03 mol/l |
| Class | Soluble |
| Log S (Ali) | -3.15 |
| Solubility | 5.61e-01 mg/ml ; 7.10e-04 mol/l |
| Class | Soluble |
| Log S (SILICOS-IT) | 0.30 |
| Solubility | 1.59e+03 mg/ml ; 2.01e+00 mol/l |
| Class | Soluble |
| **Pharmacokinetics** | |
| GI absorption | Low |
| BBB permeant | No |
| P-gp substrate | No |
| CYP1A2 inhibitor | No |
| CYP2C19 inhibitor | No |
| CYP2C9 inhibitor | No |
| CYP2D6 inhibitor | No |
| CYP3A4 inhibitor | No |
| Log Kp (skin permeation) | -12.81 cm/s |
| **Drug-likeness** | |
| Lipinski | No; 3 violations: MW>500, NorO>10, NHorOH>5 |
| Ghose | No; 4 violations: MW>480, WLOGP<-0.4, MR>130, #atoms>70 |
| Veber | No; 2 violations: Rotors>10, TPSA>140 |
| Egan | No; 1 violation: TPSA>131.6 |
| Muegge | No; 5 violations: MW>600, XLOGP3<-2, TPSA>150, H-acc>10, H-don>5 |
| Bioavailability Score | 0.17 |

| **Medicinal Chemistry** | |
|---|---|
| PAINS | 0 alert |
| Brenk | 1 alert; peroxide |
| Lead-likeness | No; 2 violations: MW>350, Rotors>7 |
| Synthetic accessibility | 8.18 |

**Recognition of Drug targets:** It is a type of study used in determining the interacting profile of CPX-CHT-PECagainst therapeutic targets that have immense pharmacological perspectives, It is important to precisely identify the potential therapeutic targets that CPX-CHT-PEC can effectively restrain at micromolar concentrations. The model for humans (*Homo sapiens*) showed the blocking effects of CPX-CHT-PEC in context of targets including Family A G protein-coupled receptor (33.3%), Kinase (26.7%), Electrochemical transporter (13.3%), Protease (20%), and Hydrolase (6.7%) (**Figure 4A**). The model of mouse (*Mus musculus*) model also had the blocking effects of CPX-CHT-PEC against Family A G protein-coupled receptor (53.3%), Kinase (6.7%), Electrochemical transporter (6.7%), Unclassified protein (6.7%), Protease (20%), and Enzymes (6.7%) (**Figure 4B**). The model of rat (*Rattus norvegicus*) showed the inhibitory activities of CPX-CHT-PEC against Family A G protein-coupled receptor (33.3%), Ligand-gated ion channel (20%), Voltage-gated ion channel (6.7%), Electrochemical transporter (6.7%), Enzyme (6.7%), Kinase (6.7%), and Hydrolase (6.7%) (**Figure 4C**). The obtained results strongly substantiated the potential interaction of this small molecule for potential applications in colorectal cancer, indicating its ability to interact with multiple targets (primarily with Family A G protein-coupled receptor).

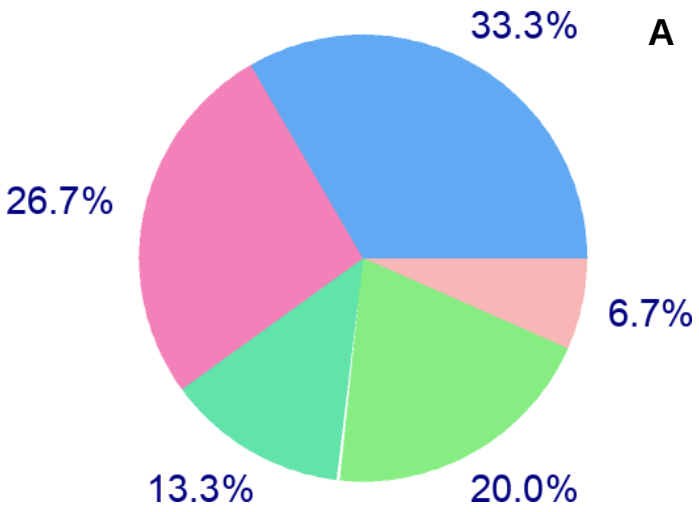


**Coupled receptor Family a G protein** (33.3%), **Kinase** (26.7%), **Electrochemical transporter** (13.3%), **Protease** (20%), **Hydrolase** (6.7%)

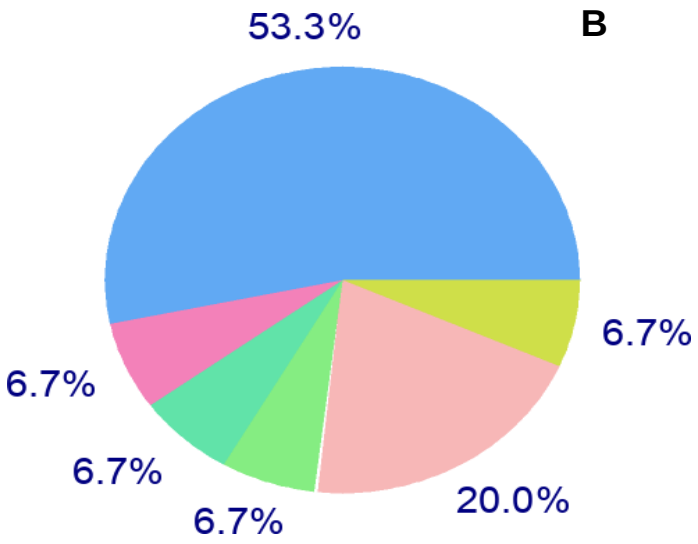


**Coupled Receptor of Family A G protein** (53.3%), **Kinase** (6.7%), **Electrochemical transporter** (6.7%), **Unclassified protein** (6.7%), **Protease** (20%), **Enzymes** (6.7%)


**Coupled receptor of Family A G protein** (33.3%), **Ligand-gated ion channel** (20%), **Voltage-gated ion channel** (6.7%), **Electrochemical transporter** (6.7%), **Enzyme** (6.7%), **Kinase** (6.7%), **Hydrolase** (6.7%)

**Figure 4.**Predicted therapeutic targets of CPX-CHT-PEC for (A) Human, (B) Mouse, and (C) Rat.

## CONCLUSION

The *in-silico* study indicated the emerging role of novel CPX-CHT-PEC in the management of colon cancer by promisingly inhibiting the molecular target galectin-3. CPX-CHT-PEC complex expressed significantly high inhibition (Gscore of -11.856 Kcal/mol) against the target galectin-3 by interacting with amino acid residues GLU165, ASN174, GLY182, and GLU184 by forming 8 hydrogen bonds via hydroxyl, amine, and carbonyl groups. Also, a non-hydrogen bonding (π-π stacking) was observed through amino acid residue TRP181 via aromatic component of the structure, suggesting a strong interaction and therefore the coexisting expression of associated pharmacotherapeutics. In the context of colon cancer targeting, this *in silico* study suggest that pharmacodynamics, pharmacokinetics, bioavailability, target identifiers, and drug-likeness properties of the CPX-CHT-PEC complex are beneficial to act as a perfect candidate against colon cancer cells.

Therefore, this study substantiates the potential for developing a lead compound and introduces new opportunities for scientists, clinicians, chemists, and other scientific professionals in addressing evolving challenges in chemotherapy.

**ACKNOWLEDGEMENTS**

The authors are highly thankful to Mahajyoti Fellowship from Government of Maharashtra and to the College management and Principal for providing the research facilities.

**REFERENCES**

1. Liu F. T., and Rabinovich G. A. *Nat. Rev. Cancer*, **2005**, *5*, 29.
2. Jiang S.S., Weng D. S., Wang Q. J., Pan K., Zhang Y. J., and Li Y. Q. *J. Transl. Med*., **2014**, *12*,
3. Barrow H., Rhodes J. M.,and Yu L.G. *Int. J. Cancer*, **2011**, *129*, 1.
4. Fortuna-Costa A., Gomes A.M., Kozlowski E.O., Stelling M.P., and Pavão M.S. Extracellular galectin-3 in tumor progression and metastasis. *Front. Oncol*., **2014**, *4*, 138.
5. Colomb F., Wang W., Simpson D., Zafar M., Beynon R., and Rhodes J. M. *J. Biol. Chem*., **2017**, *292*, 8381.
6. Zhao Q., Barclay M., Hilkens J., Guo X., Barrow H., and Rhodes J.M..*Mol Cancer*. **2010**, *9*, 1.
7. Zhao Q., Guo X., Nash G.B., Stone P.C., Hilkens J., and Rhodes J.M. *Cancer Res*. **2009**, *69*, 6799.
8. Duckworth C.A., Guimond S.E., Sindrewicz P., Hughes A.J., French N.S., and Lian L.Y. *Oncotarget*, **2015**, *6*, 23671.
9. Chen C., Duckworth C.A., Zhao Q., Pritchard D.M., Rhodes J.M., and Yu L.G. *Clin. Cancer Res*., **2013**, *19*, 1693.
10. Li S., Pritchard D.M., and Yu L.G. *Cell Death Dis*., **2023**, *14*, 268.
11. Subissi A., Monti D., Togni G., and Mailland F. Ciclopirox. *Drugs*, **2010**, *70*, 2133.
12. Sonthalia S., Agrawal M., and Sehgal V. N. *Indian Dermatol. Online J*., **2019**, *10*, 481.
13. Minden M.D., Hogge D.E., Weir S.J., Kasper J., Webster D.A., Patton L., Jitkova Y., Hurren R., Gronda M., Goard C.A., and Rajewski L.G. *Am. J.Hematol*. **2014**, *89*, 363.
14. Shen T., Shang C., Zhou H., Luo Y., Barzegar M., Odaka Y., Wu Y., and Huang S. *Genes Cancer*, **2017**, *8*, 505.
15. Pushpakom S., Iorio F., Eyers P.A., Escott K.J., Hopper S., Wells A., Doig A., Guilliams T., Latimer J., McNamee C., and Norris A. *Nat. Rev. Drug Discov*., **2019**, *18*, 41.
16. Mahapatra D.K., Bharti S.K. (*CRC Press*),**2019**.
17. Mahapatra D.K., Bharti S.K. (*Taylor & Francis*),**2017**.
18. Deokar S.S., Shaikh K.S.*Biointerf. Res. Appl. Chem*.,**2022**, *12*, 7287.
19. Deokar S.S., Shaikh K.S., Chaudhari P.D., and Deokar S.S. *J Med Pharm Allied Sci*. **2022**, *11*, 4727.
20. Patel N.V., Patel J.K., Shah S.H., and Patel J.J. *Int. J. Res. Pharm. Sci*., **2010**, *1*, 94-102.
21. Asati V., Bharti S.K., Rathore A., and Mahapatra D.K. *Indian J. Pharm. Edu. Res.*, **2017**, *51*, 436.
22. Joseph T.M., Sharanya C.S., Mahapatra D.K., Suresh K.I., Sabu A., and Haridas M. *J. Sci. Indus. Res.*, **2018**, *77*, 330.
23. Chhajed S.S., Chaskar S., Kshirsagar S.K., Haldar A.G.M., and Mahapatra D.K. *Comp. Biol. Chem*., **2017**, *67*, 260.
24. Mahapatra D.K., Das D., and Shivhare R.S. *Int. J. Pharm. Sci*., Drug Res. **2017**, *9*, 139-44.
25. Singh R.K., Mishra A.K., Kumar P., and Mahapatra D.K. *Int. J. Curr. Res. Rev.*, **2021**,*13*, S189.
26. D. E. Shaw Research, Schrödinger Release (2020-3Å). Desmond molecular dynamics system. Maestro-Desmond interoperability tools.**2020**.